PCCP

Accepted Manuscript

ROYAL SOCIETY OF CHEMISTRY

www.rsc.org/pccp

PCCP

RSCPublishing

ARTICLE

Structural Evolution and Solvation of OH radical in Ionized Water Radical Cations $(H_2O)_n^+$, n = 5 ~ 8

[1]Cite this: DOI: 10.1039/xoxxoooooox

En-Ping Lu[a], Piin-Ruey Pan[a], Ying-Cheng Li[a], Ming-Kang Tsai[b], Jer-Lai Kuo[a]

Received ooth January 2012,
Accepted ooth January 2012

DOI: 10.1039/xoxxoooooox

www.rsc.org/

Structural evolution of ionized water radical cations $(H_2O)_n^+$, n = 5 ~ 8 is studied by *ab intio* methods. A structure searching method based on previous understanding of the hydrogen bond (H-bond) network in neutral and protonated water cluster is found to be effective to cover a wide range of structural isomers of $(H_2O)_n^+$. With these local minima, we can analyze both the size and temperature dependence of the structure of $(H_2O)_n^+$ and solvation of OH radical. Agreements between our calculated IR spectra with experimental data in the free OH stretching region confirms that OH radical preferred to stay on the terminal site of the H-bond network for n=5 and n=6. Furthermore, we found OH radical begin to form H-bond with water molecules as a H-bond donor in n=7 and 8. Vibrational signatures of fully solvated OH were found to locate at 3200 ~ 3400 cm^{-1} coincides with the additional peaks found in previous experimental data obtained by Mizuse and Fujii.

I. Introduction

Neutral and ionic water clusters have been the center of many spectroscopic and theoretical studies for their important roles to understand the nature of H-bonding, solvation of H^+ and OH^- and proton transfer processes in aqueous media.[1–81] Water radical cations, $(H_2O)_n^+$, however, received less attention and only become accessible by spectroscopic investigations in the last 5 years. Since then, these radical cations have been studied extensively to gain a better understanding on the H-bond network of $(H_2O)_n^+$ with a hope to shed a new insights to the radiation-initiated ionization processes in liquid water and aqueous solutions instead of directly studying such complicated process.[15–29] Since 2009, structures of small-sized ionized water clusters have been characterized by many experimental and theoretical groups.[19–29] One of the main focuses is the relative stability between proton-transferred (PT) and hemi-bonded (Hm) structures. IR spectra from Johnson's group have determined that dimer cation is a complex consisted of H_3O^+ and OH radical.[21] On the theoretical end, it is known that many density functional methods often suffer from self-interaction errors, and symmetry-breaking in such open-shell doublet systems. Thus, many theoretical works have been devoted to find suitable and economical *ab initio* methods to study these cation clusters.[19,25–27,82]

To link to ionization processes in condensed phases, it is very important to go beyond dimer and study structure of larger $(H_2O)_n^+$. Although production of $(H_2O)_n^+$ has been demonstrated in early experimental studies by Nishi's group[13], direct structural information about $(H_2O)_n^+$ was not realized until Fujii's group obtained IR spectroscopies of $(H_2O)_n^+$, n ≤ 3-11[23]. Mizuse and Fujii analyzed and compared IR spectra of $(H_2O)_n^+$ to their protonated counterparts $H^+(H_2O)_n$ and found evident structural similarity between $H^+(H_2O)_n$ and $(H_2O)_n^+$. Furthermore, for n ≤ 6 a new vibrational peak in $(H_2O)_n^+$ at 3540 cm^{-1} was assigned to free O-H stretch mode of OH radical. These IR spectral features suggest the structure of $(H_2O)_n^+$ can be understood as $(H_3O)^+..OH..(H_2O)_{n-2}$ and OH radical is preferred to sit on the terminal sites of the H-bond network. Availability of these experimental data has thus stimulated a few theoretical works to study the structural evolution and solvation of OH radical in trimer and pentamers.[22,29,74–76]

For even larger clusters, vibrational signature of free OH of the radical begin to disappear at size n = 6 and by n ≥ 7 this vibrational signature has significant overlap with high frequency edge of H-bonded OH stretch of neutral water molecules. Therefore, the solvation of OH radical in the H-bond network of $(H_2O)_{n\geq7}^+$ cannot be easily derived from experimental data alone. Intuitively, OH radical is known to be a weaker H-bond acceptor (compare to H_2O), so in small-sized ionized water clusters, OH radical is energetically preferred to be excluded from the first solvation shell of H_3O^+. It is therefore reasonable to expect OH radical to reside on second solvation for n ~ 5. As the size of the clusters increases (that is by including additional H_2O to form more complex H-bond network), the fact OH is a strong donor[77–79] should emerge. This property of OH radical would promote OH to donate H-bond to other water molecules. Given these two competing factors and the formation of more complex H-bond network intrinsic to large water clusters, the solvation of OH radical in large-sized becomes a challenging task.

In addition to the lack of direct experimental evidence in the well resolved free OH stretching region, co-existence of multiple isomers is expected (especially for n ≥ 5) under experimental conditions.[23] In 2013, Mizuse and Fujii compared spectra of $(H_2O)_n^+$, n<8 with and without Ar attachment and characterized isomeric structures.[28] They also attempted to address the influence of temperature on the structure of $(H_2O)_n^+$ and determine the number of water molecules between H_3O^+ and OH radical. On the theoretical end, the enormous number of possible isomers hinders an extensive search with high-level *ab initio* methods. Recently, Do and Besley[29] carried out an extensive search for global minima of $(H_2O)_n^+$, n ≤ 9 based on B3LYP/6-31+G* and basin-hoping algorithm. They further re-optimized selected isomers with MP2 and other high-level *ab initio* methods to find that PT structures are more stable than the Hm structures. Low-energy minima they found yield spectra in the free OH stretching region comparable to

experimental data. However, spectral features in the H-bonded OH stretching (that is below 3400 cm^{-1}) were not studied.

In this work, we aim to understand the solvation of OH radical in the H-bond network of $(H_2O)_n^+$ by an *ab initio* based theoretical approach. First, we carried out an extensive search for different conformations of $(H_2O)_n^+$, $n \leq 8$ using a different approach from that of Do and Besley. Our method is based on the knowledge of neutral and protonated water clusters and chemical properties of $(H_2O)_n^+$. We collected many structurally distinct isomers and confirmed that we have the same global minimum for $n \leq 6$ as reported by Do and Besley. In addition, we identified energetically more stable isomers for $n > 7$ clusters. With these collected structures, we simulated temperature dependent properties such as the structural evolution and solvation of OH radical in $(H_2O)_n^+$. New vibrational peaks seen in experimental data in the H-bonded OH stretching regions (3200 ~ 3400 cm^{-1}) were assigned to be the vibrational signatures of fully solvated OH radical.

II. Methodology

In this work, initial structures of cationic water cluster were generated either by removing an electron from the stable minimum of neutral water clusters or by removing a H-atom from the stable minimum of protonated water clusters. The former scheme mimicked the ionization process from stable forms of neutral clusters and the later scheme was based on the similarity in H-Bond network of $H^+(H_2O)_n$ and $(H_2O)_n^+$ suggested by IR spectra from Fujii's group. The underlying concept of our structural searching method is based on our previous studies on neutral[80] and protonated[64] water clusters. The validity of this approach can be tracked by to the work by Singer *et al* on comparing the H-bond network of $(H_2O)_8$ and $OH(H_2O)_7$.[77] They found the relative stability of different isomers of $(H_2O)_8$ and $OH(H_2O)_7$ is governed by the same H-bond pattern. Furthermore, in our previous studies on $H^+(H_2O)_n$ and $(H_2O)_n$ the energy landscape of these clusters were extensively searched with a combination of genetic algorithm, empirical models and *ab initio* methods.[64,80,81] We are confident that we are able to locate a wide range of structural isomers of $H^+(H_2O)_n$ and $(H_2O)_n$.

Geometry optimizations with BH&HLYP and B3LYP using Gaussian 09 program package[89] were carried out to refine structure of $(H_2O)_n^+$, n=5~8. Since BH&HLYP functional gave a reasonably close result to the high-level calculations at CCSD(T)/CBS for cationic water dimer system being reported by several studies,[19,27] geometric optimization from initial structures were first carried out with BH&HLYP/aug-cc-pVDZ basis set. In order to compare with the results reported by Do and Besley[29], additional geometry optimizations at B3LYP level with 6-31+G* basis set were also performed.

A significant number of optimized structures were archived throughout the process. We should note here that some of the local minima we encountered in this process likely represent very similar region of the PES and these duplicate structures, if not removed, would make the simulation results unreliable as their contributions could artificially be amplified. In this work, the ultrafast structure recognition (USR) algorithm[83,84] is used to filter out duplicate structures. Under USR algorithm, the similarity of two structures is measured by an index (we called similarity index) with values ranging from 0 to 1. A value of 0 indicates that two structures are totally different, whereas the other extreme (when similarity index is equal to 1) represent a perfect match. In our study, a newly discovered structure is deemed as a duplicate if the similarity index to any of the existing structures in the archive exceeds a threshold of 0.95. For the optimized structures, harmonic frequency calculations were also carried out to confirm these structures are true energy minima.

Our approach is shown to be quite effective to find the minimum structure as most of our initial structures resulted in stable minima of $(H_2O)_n^+$ clusters Furthermore, since our initial structures inherit different types of H-bond networks in neutral and protonated water clusters; both energetically favourable and unfavourable structural isomers will be captured and preserved in our scheme. To prove the efficiency of our approach, we compared our results with those obtained by Do and Besley on the PES of B3LYP/6-31+G* and found that we have the same global minima for $n \leq 6$. For larger ones (that is n=7 and 8), we found energetically more stable isomers. Another advantage of our method over Basin-Hopping algorithm is that we are not limited to low-energy regions. The isomers we found cover an energy range of more than 10 kcal/mol. Thus, we believe that a more complete coverage of the rough energy landscape of $(H_2O)_n^+$ was achieved.

III. Results and discussion

Structure and Energetics of $(H_2O)_n^+$, n = 5 – 8

We located 34, 97, 309 and 606 structurally distinct isomers for $(H_2O)_n^+$, n=5, 6, 7 and 8 respectively. Relative energetics (with zero-point energy correction) of these stable isomers of $(H_2O)_n^+$ described by BH&HLYP/aug-cc-pVDZ are shown in Fig. 1. It is clear that proton-transferred (PT) isomers (labeled as black circles) are energetically more stable than the Hemi-bonded (Hm) isomers (labeled as orange squares). For n=5~8, the relative energies of the most stable PT and Hm structures are consistently differed by more than 10 kcal/mol – a trend confirmed by CCSD(T) for n=2, 3 and 4 in previous theoretical works.[27,90] Re-optimization of these structures using CCSD(T) with large basis set is beyond our current computational capacity, but in the future it would be important to check if this energetic difference can be confirmed by high-level *ab intio* methods.

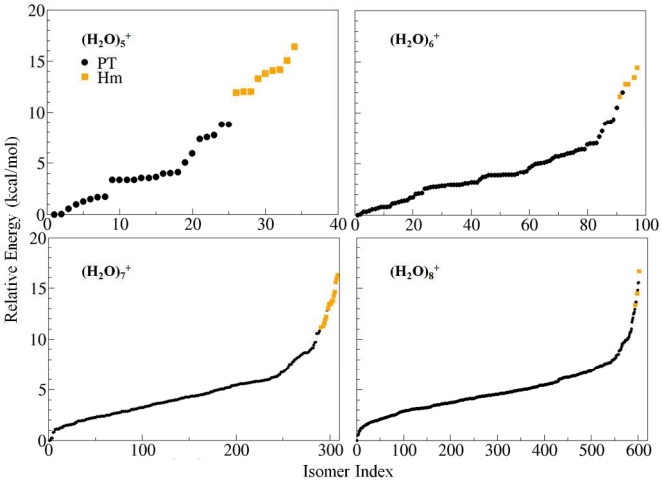

Fig. 1 Relative energy of the stable isomers of $(H_2O)_n^+$ found by our searching method with BH&HLYP/aug-cc-pVDZ. Proton-transferred (PT) isomers are black-coded circles and Hemi-bonded (Hm) isomers are shown as brown squares. A much clear figure, which contains topology information, can be found in supporting information.

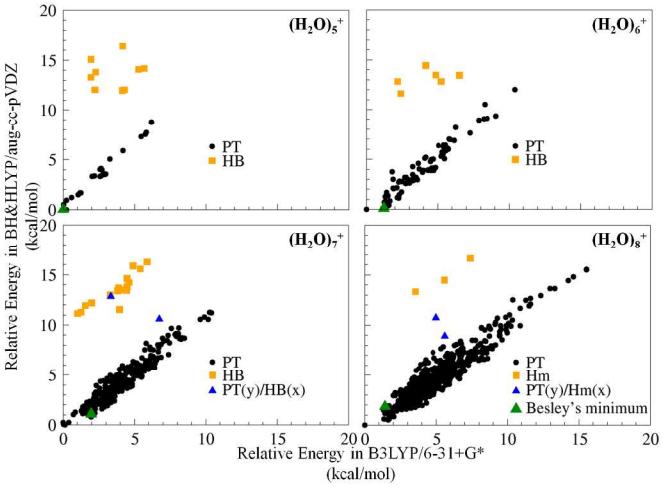

Fig. 2 Comparison on the relative energetics of the isomers of $(H_2O)_n^+$, n=5-8 described by BH&HLYP/aug-cc-pVDZ (y-axis) and B3LYP/6-31+G*(x-axis). PT and Hm structures are shown in black and brown. Global minima found by Do and Besley is shown in green. PT structures that turn into Hm are shown in blue triangle.

In order to compare with previous work by Do and Besley, we re-optimized all stable isomers we found with B3LYP/6-31+G*. The comparison on the relative energetics with these two exchange and correlation functionals is depicted in Fig. 2 with the most stable structures found by Do and Besley highlighted in green. Even using B3LYP as a standard for comparison, it is obvious that our searching method can identify energetically more stable isomers for n=7 and n=8. This is clear evidence that our search scheme works well in exploring low energy region of the PES of $(H_2O)_n^+$. Furthermore, it is also obvious from Fig. 2 that B3LYP/6-31+G* artificially favors the energetics of Hm structures – a deficiency noted in several studies on dimer and trimer[19,25,27]. It is also worth mentioning that some of the PT isomers (stable under BH&HLYP/aug-cc-pVDZ) were re-optimized into Hm forms by B3LYP/6-31+G* and they are shown as blue triangles. Since our approach is motivated by the connection between $(H_2O)_n^+$ to their neutral and protonated counterpart, its validity will not be linked to the success/failure of certain exchange and correlation functionals under DFT.

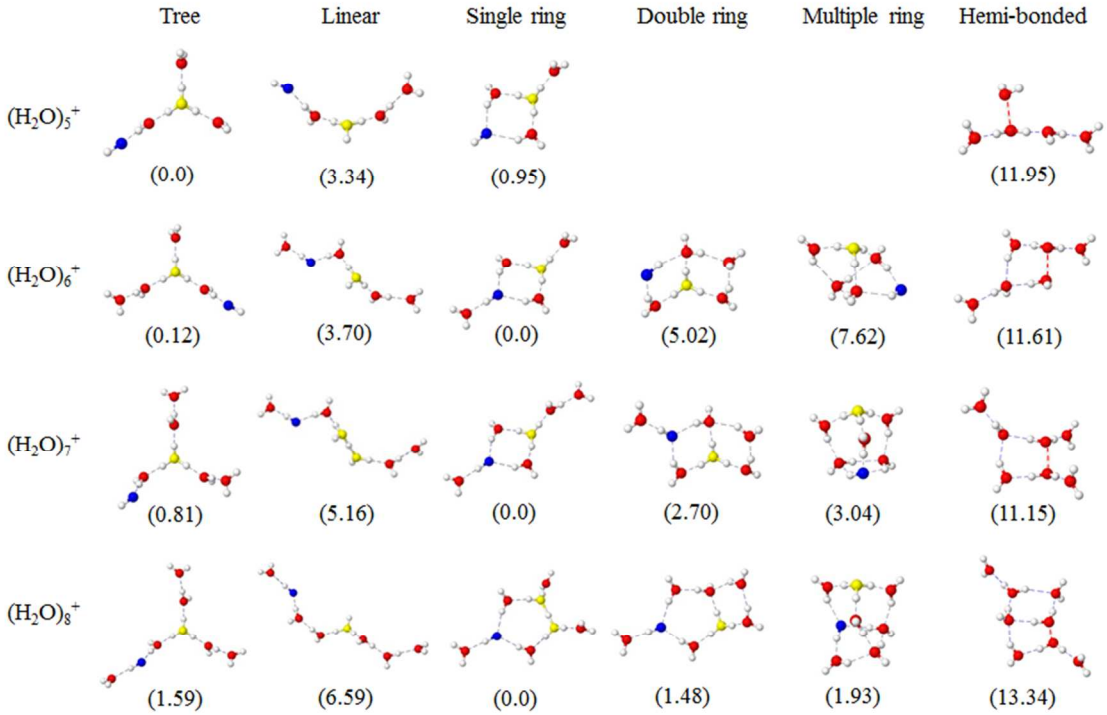

Fig. 3 The most stable structures of $(H_2O)_n^+$ in different topological groups. To guide the eyes, the O atom of H_3O^+, OH radical and H_2O are shown in yellow, blue and red. The relative energies with ZPE correction (in kcal/mol) are shown in parenthesis. The coordinate of those structures and comparison on the relative energetics among several DFT functionals and MP2 can be found in supporting information.

Due to the large number of stable local minima we have found, it is impossible to show all the structures in the manuscript. For simplicity and for bookkeeping purposes, we have categorized all the structures by their topologies: linear, tree, single-ring, double-ring and multiple-rings. In Fig. 3, only some of the representatives – the most stable isomer in each topological group – are shown. Their ZPE corrected relative energies by BH&HLYP/aug-cc-pVDZ are shown in parentheses. Comparison on the relative energetics among several DFT functionals and MP2 can be found in supporting materials.

For n=5, only three types of topologies (tree/branch, single ring and linear forms) were found and the most stable isomer is a tree structure. The 4th most stable isomer has a 4-member ring structure with ~ 1 kcal/mol higher than the global minimum. For n=6, a single-ring structure (with a 4-member ring) is the most stable isomer with a very small margin and there are many tree structures that dominate the low-energy region (see Fig. 1). At this size, we found a few double-ring and triple-ring structures, but their relative energies are much higher (5.02 kcal/mol and 7.62 kcal/mol respectively). For n=7, four out of the five lowest energy minima have single-ring with both 4- and 5-member ring. Within 2 kcal/mol,

one can find a mixture of single-ring and tree structures. The competition between these two types of isomers gives rise to a structural change at low temperature – a point we will discuss latter. For n=8, single-ring structures (with different ring sizes) dominate the low-energy region (below 1.59 kcal/mol). The most stable double-ring structure is ranked 18th with 1.48 kcal/mol higher in energy. The most stable branch/tree is ranked 40th with 1.93 kcal/mol higher in energy. While the energies of double- and multiple-ring structures seem to be comparable to tree isomers, they are not competitive in free energy even at elevated temperature.

Temperature Dependence on the Population of isomers & Coordination number of OH

To get a more quantitative analysis on the contributions of all the isomers, one can engage quantum harmonic superposition approximation (Q-HSA) to calculate populations of different groups of isomers at finite temperature.[85,86] Under this scheme, the total partition function ($Z(\beta)$) is taken as a direct sum of contributions from all local minima. Within harmonic approximation, the contribution from isomer *a* can be written as

$$Z_a(\beta) = \exp(-\beta E_a)\prod_f \frac{\exp(-\beta\hbar\omega_f^a/2)}{1-\exp(-\beta\hbar\omega_f^a)},$$

where β=(1/k_BT), E_a is the electronic energy, and ω_f^a is the *f*-th vibrational frequency of isomer *a*.

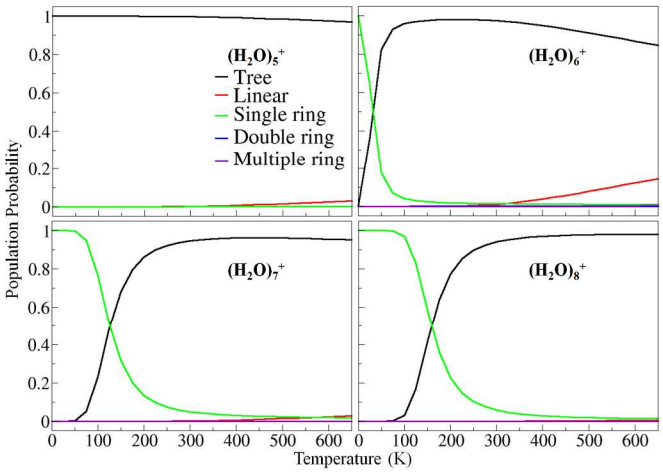

Fig. 4 Temperature dependence of the population of different topological groups for $(H_2O)_n^+$, n=5~8. The population of each topological group is obtained by considering all the possible isomers in each group In n=6 to 8, single-rings are energetically more favourable, but as temperature increases tree structures takes over. The relevant of these structural changes with IR spectra (shown in Fig.6) is presented in main text.

With the above-mentioned scheme, the population of each type of topological group can be calculated by including all isomers we found and the results are compiled in Fig.4. Similar to the notion learnt from browsing through low-energy minima of $(H_2O)_5^+$, tree structures are found to dominate the entire temperature range we examine (that is up to ~ 650K). This prediction is consistent with experimental IR data by Fujii's group that spectra of $(H_2O)_5^+$ with and without Ar attachments do not show any significant spectroscopic features of populating other types of isomers.

For n=6, the most stable form is single-ring, but as temperature increases above 50K tree structures take over. We also should point out that hexamer has several tree structures with minor differences in their IR spectral features. Consistent with our calculated results, Mizuse and Fujii observed subtle changes of the free OH stretching modes of different tree isomers between 3550 and 3570cm^{-1} in their Ar-tagged $(H_2O)_6^+$. In our calculations, linear structures manage to gain marginal percentage ~ 400K, however, this is a temperature region too high to be observed by infrared pre-dissociation (IRPD) spectra.

The morphology of $(H_2O)_7^+$ and $(H_2O)_8^+$ show similar temperature dependence – that is single-ring isomers dominates low temperature region (up to 100K for n=7 and up to 150K n=8) before tree structures take over and become dominating species at ~ 200K. These structural/isomer changes occur in a temperature range that is most likely accessible by IRPD. In the next section, we will discuss IR spectra of $(H_2O)_7^+$ and compare with experimental data obtained by Mizuse and Fujii. We should note here that even though our calculations suggest that temporal change will be more significant in n=8, Ar-tagged $(H_2O)_8^+$ is not yet available for comparison.

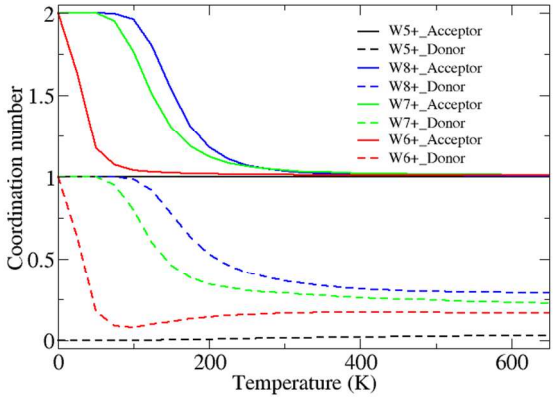

Fig. 5 Temperature dependence of the coordination number of OH radical in $(H_2O)_n^+$, n=5~8.

The solvation of OH radical moiety in $(H_2O)_n^+$ is yet another interesting issue to be examined. With Q-HSA, we are able to analyze the temperature dependence of the coordination number of OH radical in $(H_2O)_{5\sim8}^+$ and the results are shown in Fig. 5. For $(H_2O)_5^+$, the dominance of tree structure with OH radical at terminal site is consistent with coordination nature of OH radical as single-acceptor throughout the entire temperature range. For $(H_2O)_6^+$, OH radical in single-ring structure is a single-donor and double-acceptor (representative structures can be found in Fig.3). As temperature rises, the coordination number of OH radical quickly drops and stabilizes at ~ 1.2 at T≥200K. At this temperature range, tree structures begin to take over, but OH radical does not go to the terminal site completely (as the averaged possibility as donor remains at ~20%). Thus, we shall expect some OH radical to form H-bonds (as both the donor and acceptor) with other water molecules. For $(H_2O)_7^+$ and $(H_2O)_8^+$, single-ring structures survive to T~200K, thus we can see that the coordination number of OH radical remains very high. This finding is an encouraging indication that suggests fully solvated OH radical should make reasonable contributions to the experimental IR spectra in the H-bonded OH stretch region. In the next section, we will come back to this point.

IR Spectra

Under Q-HSA scheme, temperature-dependent IR spectra can be computed by summing up the contributions from all isomers with proper statistical weights using the following form: $I_{\text{total}}(\omega,T) = \sum_a I_a(\omega)P_a(T)$, where $P_a(T)=Z_a(\beta)/Z(\beta)$ and $I_a(\omega)$ is the spectrum of isomer a with the harmonic frequencies scaled by a factor of 0.920.[19] In addition, the spectra are convoluted with a homogeneous width proposed by Takahashi *et al* based the vibrational decay lifetime (Γ) of the OH stretching modes.[87,88] The width we used can be written as $\Gamma = \alpha(\Delta\omega)^{\beta} = \alpha(\omega_{\text{free OH}} - \omega_{\text{H-bonded OH}})^{\beta}$, where Δω is the red shift of the H-bonded OH band peak with respect to the free OH peak of the experimental spectra of $(H_2O)_n^+$. The parameters α and β were determined by using the least-squares fitting procedure to fit experiment data from Fujii's group. The parameters table for each size can be found in supporting information.

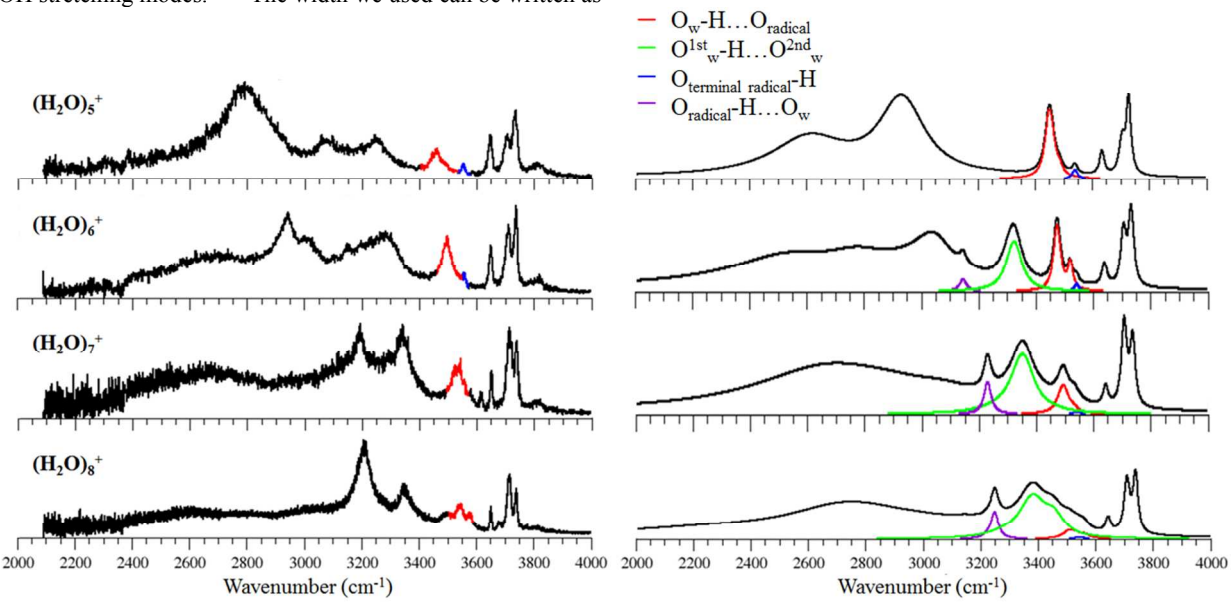

Fig. 6 Experimental and simulated IR spectrum of water cluster cation. Simulated spectra were extracted based on thermal condition at T=200K. The decomposition of vibration peaks into blue (the stretch of terminal OH) and red (the stretch of water to terminal OH) is based on the assignments of Mizuse and Fujii. In our calculations, we found two new bands: the stretch of 1st solvation shell to 2nd shell is shown in green and the stretch of solvated OH is in purple.

To understand spectra of neat $(H_2O)_n^+$ by Fujii's group[23], we simulate IR spectra of $(H_2O)_n^+$ based on population of different isomers at 200K and compare them with experimental data in Fig.6. Vibrational bands above 3600cm^{-1} come from free OH stretching modes of water molecules with different coordination numbers. These modes have been used extensively to identify the morphological development in water clusters.[23] Therefore, consistency between experimental data and our calculated spectra in this region indicates that the topology of the H-bond network of $(H_2O)_n^+$ is well described in our simulations. The stretching mode of free OH of the radical has been assigned to be the band at ~ 3550 cm^{-1} by Fujii.[28] These bands are highlighted in blue in both experimental and calculated spectra. Similar to experimental data, these blue bands in our simulation start to overlap with red bands (assigned to O_w-H…$O^{terminal}{}_{radical}$ by Fujii) at ~ 3500 cm^{-1} for n ≥ 6.

In addition to overall agreements between experimental and simulated spectra, our calculations offer some advantages – that is we can keep track of the contribution of each isomer in our simulated spectra. Contributions from different OH stretching modes can be unambiguously assigned. Our interpretation of the nearly disappearance of free OH band of the radical at n ≥ 7 is mainly due to the decline in their related populations. The decrease in intensity of the red bands is also a consistent indication that OH radical begins to function as H-bond donors and form more complex H-bond network.

In experimental spectra of $(H_2O)_6^+$, a relatively broad absorption between 3100 and 3400cm^{-1} was observed. Moreover, in $(H_2O)_7^+$ and $(H_2O)_8^+$, two separated bands emerge at 3200 cm^{-1} and 3350 cm^{-1}, respectively. According to our calculations, vibration modes around 3400cm^{-1} (shown in green) can be attributed to O_w-H…O_w between water molecules in the first and second solvation shell of H_3O^+. Increase in intensity of these green bands is due to the complete second hydration shell. The vibrational signature to account for fully solvated OH radicals is found to be a band ~3200cm^{-1}. In our calculations, we highlighted the H-bonded OH stretching modes in $O_{radical}$-H…O_w as the purple bands. These purple bands occur at below 3200cm^{-1} in $(H_2O)_6^+$. As size of cation clusters grow, these purple bands blueshifts to be slightly above 3200cm^{-1}. Furthermore, the intensity of both the purple bands gradually increase from n=6 to n=8 indicating the percentage of fully solvated OH increases. For n=8, one can clearly see that OH radical are more likely to be embedded in H-bonded network as a donor and acceptor than stay on the terminal site (characterized by the blue bands).

To access the effects of temperature on the structural changes of $(H_2O)_n^+$, one can compare spectra of neat and Ar-tagged $(H_2O)_n^+$ because the weaker binding energy of Ar to $(H_2O)_n^+$ gives a lower upper limit of the vibrational temperature of Ar-tagged $(H_2O)_n^+$. Mizuse and Fujii compared experimental spectra of neat and Ar-tagged $(H_2O)_7^+$ and noticed several significant spectral changes. In Fig. 7, we compare our simulated spectra at 75K and 200K to experimental spectra of Ar-tagged and neat $(H_2O)_7^+$ respectively. It is clear that the main difference between simulated spectra at 75K and 200K is the increase in intensity of the purple (due to fully solvated OH) band and decrease of the green (due to $O^{1st}{}_w$-H…$O^{2nd}{}_w$) band. The same notion can be found by comparing experimental spectra of Ar-tagged and neat $(H_2O)_7^+$. Consistency in these IR spectral features in H-bonded OH stretching modes between experimental data and our predictions based *ab initio* calculations not only grant us an evidence of fully solvated OH

radical but also demonstrate the importance of proper sampling of different conformation of water radical cation clusters.

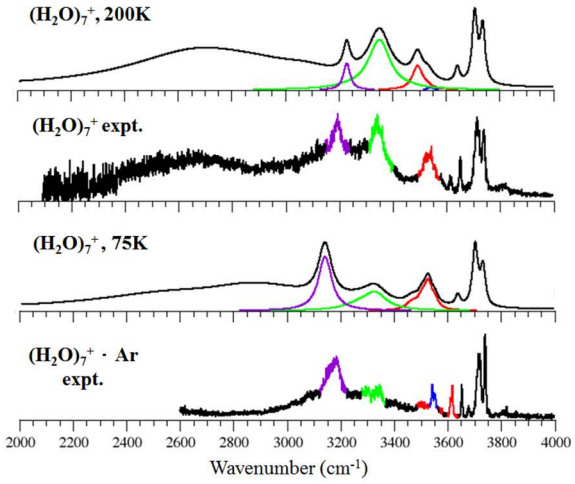

Fig. 7 Experimental spectra of neat and Ar-tagged $(H_2O)_7^+$ are compared against our simulated spectra of $(H_2O)_7^+$ at 200K and 75K respectively. Color coding of vibrational bands followes the same defintions used in Fig. 6.

Conclusions

In this study, we reported an extensive search of the conformational isomers of $(H_2O)_n^+$, n=5-8. By comparing with previous global search using basin-hopping algorithm by Do and Besley, we demonstrated our approach based on previous understanding of the H-bond network of neutral and protonated water cluster is an efficient and effective method. With BH&HLYP with aug-cc-pVDZ, we were able to locate a few hundred stable isomers. Proton-transferred (PT) structures are found to be energetically more stable than their hemi-bonded (Hm) counterparts by ~ 10 kcal/mol for up to n=8. While accuracy of BH&HLYP/aug-cc-pVDZ remains to be tested for $n \geq 5$, the stable isomers were found can be further tested by high-level of *ab intio* methods to validate the performance of density functional methods. The stable local minima we found enable us to get a statistical average mimicking the ensemble average near experimental conditions. A consistent picture on the structural and temporal evolution of $(H_2O)_{5\text{-}8}^+$ has been obtained by comparing to the free OH stretching modes in IRPD. Furthermore, our DFT calculations show that OH radical begin to form H-bond with water molecules at n=7 and 8. Vibration signatures of fully solvation OH radical at 3200 ~ 3400 cm^{-1} are proposed and our findings agrees well with experimental spectra of $(H_2O)_n^+$ and $H^+(H_2O)_n$.

Acknowledgements

The authors are grateful to the financial support from Ministry of Science and Technology of Taiwan (Grant 101-2113-M-003-003-MY2 and 101-2113-M-001-023-MY3) and Academia Sinica. Computational resources are in part supported by National Center for High Performance Computing. We would like to thank Dr. Kaito Takahashi for various insightful discussions, Mr. Cheng-Hao Wu for sharing his program to visualize cluster structures, and Dr. Kenta Mizuse and Prof. Asuka Fujii for providing us experimental data for comparison.

Notes and references

[a] Institute of Atomic and Molecular Sciences, Academia Sinica, Taipei 10617, Taiwan.
[b] Department of Chemistry, National Taiwan Normal University, Taipei 10677, Taiwan.

† Electronic Supplementary Information (ESI) available: [details of any supplementary information available should be included here]. See DOI: 10.1039/b000000x/

References

1. B. C. Garrett, D. A. Dixon, D. M. Camaioni, D. M. Chipman, M. A. Johnson, C. D. Jonah, G. A. Kimmel, J. H. Miller, T. N. Rescigno, P. J. Rossky, S. S. Xantheas, S. D. Colson, A. H. Laufer, D. Ray, P. F. Barbara, D. M. Bartels, K. H. Becker, K. H. Bowen, S. E. Bradforth, I. Carmichael, J. V Coe, L. R. Corrales, J. P. Cowin, M. Dupuis, K. B. Eisenthal, J. A. Franz, M. S. Gutowski, K. D. Jordan, B. D. Kay, J. A. LaVerne, S. V Lymar, T. E. Madey, C. W. McCurdy, D. Meisel, S. Mukamel, A. R. Nilsson, T. M. Orlando, N. G. Petrik, S. M. Pimblott, J. R. Rustad, G. K. Schenter, S. J. Singer, A. Tokmakoff, L.-S. Wang, C. Wettig, and T. S. Zwier, *Chem. Rev.*, 2005, **105**, 355–89.
2. E. Alizadeh and L. Sanche, *Chem. Rev.*, 2012, **112**, 5578–602.
3. C. Silva, P. K. Walhout, K. Yokoyama, and P. F. Barbara, *Phys. Rev. Lett.*, 1998, **80**, 1086–1089.
4. Y. Gauduel, S. Pommeret, A. Migus, and A. Antonetti, *Chem. Phys.*, 1990, **149**, 1–10.
5. C. L. Thomsen, D. Madsen, S. R. Keiding, J. Thøgersen, and O. Christiansen, *J. Chem. Phys.*, 1999, **110**, 3453-62.
6. A. Migus, Y. Gauduel, J. L. Martin, and A. Antonetti, *Phys. Rev. Lett.*, 1987, **58**, 1559–62.
7. K. Mizuse, T. Hamashima, and A. Fujii, *J. Phys. Chem. A*, 2009, **113**, 12134–41.
8. K. Mizuse, N. Mikami, and A. Fujii, *Angew. Chem. Int. Ed.*, 2010, **49**, 10119–22.
9. K. Mizuse and A. Fujii, *Phys. Chem. Chem. Phys.*, 2011, **13**, 7129–35.
10. K. Mizuse and A. Fujii, *Chem. Phys.*, 2013, **419**, 2–7.
11. V. Buch, S. Bauerecker, J. P. Devlin, U. Buck, and J. K. Kazimirski, *Int. Rev. Phys. Chem.*, 2004, **23**, 375–433.
12. U. Buck and F. Huisken, *Chem. Rev.*, 2000, **100**, 3863–90.
13. H. Shinohara, N. Nishi, and N. Washida, *J. Chem. Phys.*, 1986, **84**, 5561-7.
14. R. T. Jongma, Y. Huang, S. Shi, and A. M. Wodtke, *J. Phys. Chem. A*, 1998, **102**, 8847–54.
15. S. Yamaguchi, S. Kudoh, Y. Kawai, Y. Okada, T. Orii, and K. Takeuchi, *Chem. Phys. Lett.*, 2003, **377**, 37–42.
16. L. Angel and A. J. Stace, *Chem. Phys. Lett.*, 2001, **345**, 277–81.
17. P. A. Pieniazek, J. VandeVondele, P. Jungwirth, A. I. Krylov, and S. E. Bradforth, *J. Phys. Chem. A*, 2008, **112**, 6159–70.
18. Q. Cheng, F. A. Evangelista, A. C. Simmonett, Y. Yamaguchi, and H. F. Schaefer, *J. Phys. Chem. A*, 2009, **113**, 13779–89.
19. H. M. Lee and K. S. Kim, *J. Chem. Theory Comput.*, 2009, **5**, 976–81.
20. E. Kamarchik, O. Kostko, J. M. Bowman, M. Ahmed, and A. I. Krylov, *J. Chem. Phys.*, 2010, **132**, 194311.
21. G. H. Gardenier, M. A. Johnson, and A. B. McCoy, *J. Phys. Chem. A*, 2009, **113**, 4772–9.
22. E. Livshits, R. S. Granot, and R. Baer, *J. Phys. Chem. A*, 2011, **115**, 5735–44.
23. K. Mizuse, J.-L. Kuo, and A. Fujii, *Chem. Sci.*, 2011, **2**, 868-76.
24. T. L. Guasco, M. A. Johnson, and A. B. McCoy, *J. Phys. Chem. A*, 2011, **115**, 5847–58.
25. H. M. Lee and K. S. Kim, *Theor. Chem. Acc.*, 2011, **130**, 543–48.
26. M.-K. Tsai, J.-L. Kuo, and J.-M. Lu, *Phys. Chem. Chem. Phys.*, 2012, **14**, 13402–8.

27. P.-R. Pan, Y.-S. Lin, M.-K. Tsai, J.-L. Kuo, and J.-D. Chai, *Phys. Chem. Chem. Phys.*, 2012, **14**, 10705–12.
28. K. Mizuse and A. Fujii, *J. Phys. Chem. A*, 2013, **117**, 929–38.
29. H. Do and N. A. Besley, *J. Phys. Chem. A*, 2013, **117**, 5385–91.
30. S. Tomoda and K. Kimura, *Chem. Phys.*, 1983, **82**, 215–27.
31. K. Norwood, A. Ali, and C. Y. Ng, *J. Chem. Phys.*, 1991, **95**, 8029-37.
32. S. P. de Visser, L. J. de Koning, and N. M. M. Nibbering, *J. Phys. Chem.*, 1995, **99**, 15444–7.
33. R. N. Barnett and U. Landman, *J. Phys. Chem.*, 1995, **99**, 17305–10.
34. Y. V. Novakovskaya and N. F. Stepanov, *Int. J. Quantum Chem.*, 1997, **61**, 981–90.
35. Y. V. Novakovskaya and N. F. Stepanov, *J. Phys. Chem. A*, 1999, **103**, 3285–8.
36. H. Tachikawa, *J. Phys. Chem. A*, 2004, **108**, 7853–62.
37. A. Furuhama, M. Dupuis, and K. Hirao, *J. Chem. Phys.*, 2006, **124**, 164310.
38. I. B. Müller and L. S. Cederbaum, *J. Chem. Phys.*, 2006, **125**, 204305.
39. L. Belau, K. R. Wilson, S. R. Leone, and M. Ahmed, *J. Phys. Chem. A*, 2007, **111**, 10075–83.
40. Y. V. Novakovskaya, *Int. J. Quantum Chem.*, 2007, **107**, 2763–80.
41. S. Yang, S. M. Brereton, S. Nandhra, A. M. Ellis, B. Shang, L.-F. Yuan, and J. Yang, *J. Chem. Phys.*, 2007, **127**, 134303.
42. A. Furuhama, M. Dupuis, and K. Hirao, *Phys. Chem. Chem. Phys.*, 2008, **10**, 2033–42.
43. A. Kumar, M. Kołaski, H. M. Lee, and K. S. Kim, *J. Phys. Chem. A*, 2008, **112**, 5502–8.
44. G. Periyasamy, R. D. Levine, and F. Remacle, *Chem. Phys.*, 2009, **366**, 129–38.
45. P. A. Pieniazek, E. J. Sundstrom, S. E. Bradforth, and A. I. Krylov, *J. Phys. Chem. A*, 2009, **113**, 4423–9.
46. T. Jahnke, H. Sann, T. Havermeier, K. Kreidi, C. Stuck, M. Meckel, M. Schöffler, N. Neumann, R. Wallauer, S. Voss, A. Czasch, O. Jagutzki, A. Malakzadeh, F. Afaneh, Th. Weber, H. Schmidt-Böcking, and R. Dörner, *Nat. Phys.*, 2010, **6**, 139–42.
47. M. Mucke, M. Braune, S. Barth, M. Förstel, T. Lischke, V. Ulrich, T. Arion, U. Becker, A. Bradshaw, and U. Hergenhahn, *Nat. Phys.*, 2010, **6**, 143–146.
48. S. Barth, M. Oncák, V. Ulrich, M. Mucke, T. Lischke, P. Slavícek, and U. Hergenhahn, *J. Phys. Chem. A*, 2009, **113**, 13519–27.
49. M. Sodupe, J. Bertran, L. Rodrı´guez-Santiago and E. J. Baerends, *J. Phys. Chem. A*, 1999, **103**, 166–70.
50. Y. Matsuda, N. Mikami, and A. Fujii, *Phys. Chem. Chem. Phys.*, 2009, **11**, 1279–90.
51. M. Hachiya, Y. Matsuda, K.-i. Suhara, N. Mikami, and A. Fujii, *J. Chem. Phys.*, 2008, **129**, 094306.
52. L. I. Yeh, M. Okumura, J. D. Myers, J. M. Price, and Y. T. Lee, *J. Chem. Phys.*, 1989, **91**, 7319.
53. M. Okumura, L. I. Yeh, J. D. Myers, and Y. T. Lee., *J. Phys. Chem.*, 1990, **94**, 3416–27.
54. Y.-S. Wang, J. C. Jiang, C.-L. Cheng, S. H. Lin, Y. T. Lee, and H.-C. Chang, *J. Chem. Phys.*, 1997, **107**, 9695.
55. J.-C. Jiang, Y.-S. Wang, H.-C. Chang, S. H. Lin, Y. T. Lee, G. Niedner-Schatteburg, and H.-C. Chang, *J. Am. Chem. Soc.*, 2000, **122**, 1398–410.
56. Y.-S. Wang, C.-H. Tsai, Y. T. Lee, H.-C. Chang, J.-C. Jiang, O. Asvany, S. Schlemmer, and D. Gerlich, *J. Phys. Chem. A*, 2003, **107**, 4217–25.
57. M. Miyazaki, A. Fujii, T. Ebata, and N. Mikami, *Science*, 2004, **304**, 1134–7.
58. J.-W. Shin, N. I. Hammer, E. G. Diken, M. A. Johnson, R. S. Walters, T. D. Jaeger, M. A. Duncan, R. A. Christie, and K. D. Jordan, *Science*, 2004, **304**, 1137–40.
59. H.-C. Chang, C.-C. Wu, and J.-L. Kuo, *Int. Rev. Phys. Chem.*, 2005, **24**, 553–78.
60. J. M. Headrick, E. G. Diken, R. S. Walters, N. I. Hammer, R. A. Christie, J. Cui, E. M. Myshakin, M. A. Duncan, M. A. Johnson, and K. D. Jordan, *Science*, 2005, **308**, 1765–9.
61. C.-K. Lin, C.-C. Wu, Y.-S. Wang, Y. T. Lee, H.-C. Chang, J.-L. Kuo, and M. L. Klein, *Phys. Chem. Chem. Phys.*, 2005, **7**, 938–44.
62. C.-C. Wu, C.-K. Lin, H.-C. Chang, J.-C. Jiang, J.-L. Kuo, and M. L. Klein, *J. Chem. Phys.*, 2005, **122**, 074315.
63. S. Karthikeyan, M. Park, I. Shin, and K. S. Kim, *J. Phys. Chem. A*, 2008, **112**, 10120–4.
64. Q. C. Nguyen, Y.-S. Ong, and J.-L. Kuo, *J. Chem. Theory Comput.*, 2009, **5**, 2629–39.
65. K. Mizuse, A. Fujii, and N. Mikami, *J. Chem. Phys.*, 2007, **126**, 231101.
66. G. E. Douberly, A. M. Ricks, and M. A. Duncan, *J. Phys. Chem. A*, 2009, **113**, 8449–53.
67. G. E. Douberly, R. S. Walters, J. Cui, K. D. Jordan, and M. A. Duncan, *J. Phys. Chem. A*, 2010, **114**, 4570–9.
68. S. Maeda and K. Ohno, *J. Phys. Chem. A*, 2007, **111**, 4527–34.
69. Y. Luo, S. Maeda, and K. Ohno, *J. Phys. Chem. A*, 2007, **111**, 10732–7.
70. Y. Luo, S. Maeda, and K. Ohno, *J. Comput. Chem.*, 2009, **30**, 952–61.
71. C. Y. Ng, D. J. Trevor, P. W. Tiedemann, S. T. Ceyer, P. L. Kronebusch, B. H. Mahan, and Y. T. Lee., *J. Chem. Phys.*, 1977, **67**, 4235-7.
72. S. Tomoda, Y. Achiba, and K. Kimura, *Chem. Phys. Lett.*, 1982, **87**, 197–200.
73. A. Golan and M. Ahmed, *J. Phys. Chem. Lett.*, 2012, **3**, 458−62.
74. H. Tachikawa and T. Takada, *Chem. Phys.*, 2013, **415**, 76–83.
75. H. Do and N. A. Besley, *Phys. Chem. Chem. Phys.*, 2013, **15**, 16214–9.
76. M. Marciante and F. Calvo, *Mol. Simul.*, 2014, **40**, 176–84.
77. S. D. Belair, J. S. Francisco, and S. J. Singer, *Phys. Rev. A*, 2005, **71**, 013204.
78. K. S. Kim, H. S. Kim, J. H. Jang, H. S. Kim, B.-J. Mhin, Y. Xie, and H. F. Schaefer, *J. Chem. Phys.*, 1991, **94**, 2057-62.
79. Y. Xie and H. F. Schaefer, *J. Chem. Phys.*, 1993, **98**, 8829-33.
80. Q. C. Nguyen, Y. S. Ong, H. Soh, and J.-L. Kuo, *J. Phys. Chem. A*, 2008, **112**, 6257–61.
81. H. Soh, Y.-S. Ong, Q. C. Nguyen, Q. H. Nguyen, M. S. Habibullah, T. Hung, and J.-L. Kuo. *IEEE Trans. Evol. Comput.*, 2010, **14**, 419–37.
82. H. Tachikawa, *Phys. Chem. Chem. Phys.*, 2011, **13**, 11206–12.
83. P. J. Ballester and W. G. Richards, *Proc. R. Soc. A*, 2007, **463**, 1307–21.
84. P. J. Ballester and W. G. Richards, *J. Comput. Chem.*, 2007, **28**, 1711–23.
85. F. Calvo, J. P. K. Doye, and D. J. Wales, *Chem. Phys. Lett.*, 2002, **366**, 176–83.
86. D. J. Wales, Properties of Landscape. In *Energy Landscape*, 1st ed.; R. Saykally, A. Zewail, D. King, Eds.; Cambridge University Press: Cambridge, U. K., 2003; Vol. 1, p 364.
87. Y.-L. Cheng, H.-Y. Chen, and K. Takahashi, *J. Phys. Chem. A*, 2011, **115**, 5641–53.
88. M. Morita and K. Takahashi, *Phys. Chem. Chem. Phys.*, 2012, **14**, 2797–808.
89. Gaussian 09, Revision A.02, M. J. Frisch, G. W. Trucks, H. B. Schlegel, G. E. Scuseria, M. A. Robb, J. R. Cheeseman, G. Scalmani, V. Barone, B. Mennucci, G. A. Petersson, H. Nakatsuji, M. Caricato, X. Li, H. P. Hratchian, A. F. Izmaylov, J. Bloino, G. Zheng, J. L. Sonnenberg, M. Hada, M. Ehara, K. Toyota, R. Fukuda, J. Hasegawa, M. Ishida, T. Nakajima, Y. Honda, O. Kitao, H. Nakai, T. Vreven, J. A. Montgomery, Jr., J. E. Peralta, F. Ogliaro, M. Bearpark, J. J. Heyd, E. Brothers, K. N. Kudin, V. N. Staroverov, R. Kobayashi, J. Normand, K. Raghavachari, A. Rendell, J. C. Burant, S. S. Iyengar, J. Tomasi, M. Cossi, N. Rega, J. M. Millam, M. Klene, J. E. Knox, J. B. Cross, V. Bakken, C. Adamo, J. Jaramillo, R. Gomperts, R. E. Stratmann, O. Yazyev, A. J. Austin, R. Cammi, C. Pomelli, J. W. Ochterski, R. L. Martin, K. Morokuma, V. G. Zakrzewski, G. A. Voth, P. Salvador, J. J. Dannenberg, S. Dapprich, A. D. Daniels, Ö. Farkas, J. B. Foresman, J. V. Ortiz, J. Cioslowski, and D. J. Fox, Gaussian, Inc., Wallingford CT, 2009.
90. P.-R. Pan, E.-P. Lu, Y.-C. Li, J.-L. Kuo, M.-K. Tsai, *J. Phys. Chem. A*, 2014 (submitted).